ORIGINAL RESEARCH

Development of Coronary Pulse Wave Velocity: New Pathophysiological Insight Into Coronary Artery Disease

Brahim Harbaoui, MD, MS; Pierre-Yves Courand, MD, PhD; Andrei Cividjian, PhD; Pierre Lantelme, MD, PhD

***Background*—**Although aortic stiffness assessed by pulse wave velocity (PWV) is a strong predictor of coronary artery disease, the significance of local coronary stiffness has never been tackled. The first objective of this study was to describe a method of measuring coronary PWV (CoPWV) invasively and to describe its determinants. The second objective was to assess both CoPWV and aortic PWV in patients presenting with acute coronary syndromes or stable coronary artery disease.

***Methods and Results*—**In 53 patients, CoPWV was measured from the delay in pressure wave and distance traveled as a pressure wire was withdrawn from the distal to the proximal coronary segment. Similarly, aortic PWV was measured invasively when the wire was pulled across the ascending aorta; carotid–femoral PWV was also measured noninvasively using the SphygmoCor system (AtCor Medical). Mean CoPWV was 10.3±6.1 m/s. Determinants of increased CoPWV were fractional flow reserve, diastolic blood pressure, and previous stent implantation in the recorded artery. CoPWV was lower in patients with acute coronary syndromes versus stable coronary artery disease (7.6±3 versus 11.5±6.4 m/s; P=0.02), and this persisted after adjustment for confounders. In contrast, aortic stiffness, assessed by aortic and carotid–femoral PWV, did not differ significantly.

***Conclusions*—**CoPWV seems associated with acute coronary events more closely than aortic PWV. High coronary compliance, whether per se or because it leads to a distal shift in compliance mismatch, may expose vulnerable plaques to high cyclic stretch. CoPWV is a new tool to assess local compliance at the coronary level; it paves the way for a new field of research. **(*J Am Heart Assoc*. 2017;6:e004981. DOI: 10.1161/JAHA.116.004981.)**

Key Words: acute coronary syndromes • aortic stiffness • compliance • coronary artery • fractional flow reserve • plaque rupture • pulse wave velocity • stiffness

Vascular stiffness plays an important role in the pathophysiology of cardiovascular events.[1,2] Aortic pulse wave velocity (AoPWV), a marker of large artery stiffness, is a strong predictor of coronary artery disease (CAD),[3] probably because aorta conveys pulsatility to coronary vessels. The close proximity of the aorta and small arteries fuels permanent cross-talk between them.[4] Nevertheless, because of their different biomechanistic properties, a stiffness gradient is usually observed between the aorta and the peripheral arteries, leading to areas of compliance mismatch. These areas induce wave reflection, which is critical to reduce downstream pulsatility.[5] Consequently, local coronary compliance should differ from aortic compliance and may be more relevant for predicting plaque rupture.[6] However, the impact of local coronary stiffness on acute coronary events has never been studied. This is most likely because appropriate tools for assessing coronary stiffness are currently lacking.

Some attempts have been made to assess local coronary compliance surrounding a plaque using intravascular ultrasound,[7] but a global appraisal of vessel biomechanics may be more appropriate. Arterial compliance is widely assessed by measuring the speed of the pressure wave across a particular segment. This approach, known as pulse wave velocity (PWV) measurement, has been used primarily for large vessels and is currently considered the gold standard to determine aortic stiffness.[8] Some previous attempts have been made to assess coronary PWV (CoPWV) in animal studies[9] and methods papers.[10,11] However, the approaches used raise important methodological issues that preclude use in routine practice.[12] The objectives of the present study were to propose a method of CoPWV measurement that could be implemented easily during a standard coronary angiogram, allowing for

From the Cardiology Department, European Society of Hypertension Excellence Center, Hôpital de la Croix-Rousse, Hospices Civils de Lyon, Lyon, France (B.H., P.-Y.C., A.C., P.L.); CREATIS, CNRS UMR5220, INSERM U1044, INSA-Lyon, Université Claude Bernard Lyon 1, Hospices Civils de Lyon, Université de Lyon, France (B.H., P.-Y.C., P.L.).

Correspondence to: Pierre Lantelme, MD, PhD, Cardiology Department, Hôpital de la Croix-Rousse, 103 Grande Rue de la Croix-Rousse, 69004, Lyon, France. E-mail: pierre.lantelme@chu-lyon.fr

Received November 2, 2016; accepted December 6, 2016.

description of determinants, and to compare coronary and aortic compliance with respect to the patient's clinical status (ie, with acute coronary syndrome [ACS] or stable CAD).

Methods

Patients and Study Design

Patients with an ACS or stable CAD undergoing a standard coronary angiogram at the Croix-Rousse Hospital (Lyon, France) with an indication for fractional flow reserve (FFR) measurement were included in the study. The indication for FFR was based on the visual estimate of the stenosis percentage of diameter reduction (≥50%). ACS was defined by usual clinical, ECG, and troponin criteria. Stable CAD indicated stable angina or silent ischemia presenting a stenosis ≥50% on at least 1 coronary artery. Exclusion criteria were age <18 years, valvular heart disease, or the presence of decompensated heart failure. Risk factors, history of CAD or peripheral artery disease, left ventricular ejection fraction, and ongoing pharmacologic medication were obtained from the patients' medical files. Renal function was calculated according to the Modification of Diet in Renal Disease formula. Conventional blood pressure (BP) and carotid–femoral PWV were measured just before the coronary angiogram. Three BP measurements, obtained at 1-minute intervals in a reclining position after 5 minutes of rest, were averaged. Carotid–femoral PWV was measured next with a Sphygmocor device (AtCor Medical); a 0.8 scaling factor was applied to the carotid–femoral distance, as described previously.[13]

CoPWV was assessed with the ECG signal and the local pressure wire signal using a computerized algorithm in all coronary arteries undergoing FFR measurement. CoPWV was reassessed during the same procedure in a subset of patients after intracoronary injection of adenosine to evaluate CoPWV reproducibility—this short-acting drug is not expected to have any sustained effect on wave speed in humans[12]—and in a second subset of patients treated with percutaneous coronary intervention, to assess the effect of stenting as a way to validate our measurement.

Aortic PWV (AoPWV) was measured invasively using the same methodology. The study protocol received ethics committee approval (Comité de Protection des Personnes Sud-Est IV). All participants gave written informed consent to participate.

Invasive Pressure and ECG Recordings

A 0.014-mm pressure guidewire (PressureWire Aeris; St. Jude Medical) was introduced via a 5F or 6F guiding catheter. ECG (Philips) and invasive BP waveforms were acquired using RECAN software (Alpha2) via an analog/digital acquisition board (KUSB-3100; Keithley-Tektronix) at 500 Hz. CoPWV was assessed with asynchronous recordings of the ECG-BP delay at 2 different sites of the coronary segment to determine the propagation time of the pressure wave (Figure 1). Synchronized BP and ECG signals were recorded for 1-minute periods at the coronary proximal and distal levels.

The distance between the 2 positions (coronary travel distance), was assumed to be equal to the elongation of the external part of the catheter after pull-back (distal to proximal). The latter was measured with a millimeter-precision ruler (Figure 1).

Pressure, ECG Analysis, and Invasive PWV Assessment

Data analysis was performed offline using an automated customized procedure with RECAN software. To improve time resolution, the signals were resampled at 2000 Hz after interpolation using cubic splines. R wave was detected for each cardiac cycle from the ECG signal using a template-matching method after memorizing an averaged R-wave shape. The onset time of the BP rise was calculated for each cardiac cycle by adapting the intersecting tangents method,[14] as described later. When the catheter was in the proximal position, onset time was calculated as the intersection of the tangent to the BP wave at the time corresponding to the peak of the BP derivative with the horizontal line passing through

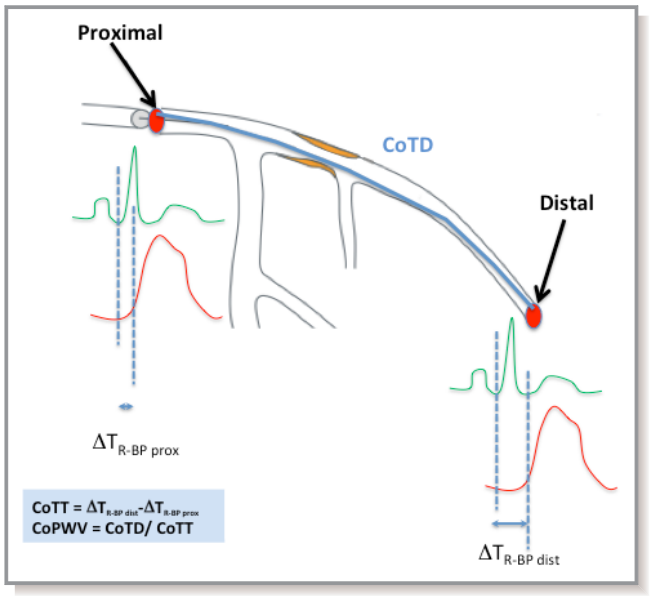

Figure 1. Illustration of the principle of coronary pulse wave velocity (CoPWV) measurement in the left descending artery. ECG–blood pressure delays ($T_{R\text{-}BP}$) are recorded successively at the distal ($T_{R\text{-}BP\ dist}$) and proximal ($T_{R\text{-}BP\ prox}$) sites. Coronary travel time (CoTT) and coronary travel distance (CoTD) allow the calculation of CoPWV.

the preceding diastolic BP (DBP) (Figure 2). When the catheter was in the distal position, the detection of onset time of the BP rise was more difficult because of a frequent premature pressure increase that impeded accurate application of the intersecting-tangents method (Figure 2). For both proximal and distal positions, a recomposed signal was created that was equal to 0 everywhere except for the period of ±10 ms centered on the onset time of BP rise, when this recomposed signal was equal to the averaged R-wave shape used to detect the R wave for each cardiac cycle (Figure 3A). A cross-correlation between the ECG and this recomposed signal was performed to calculate the delay between the R

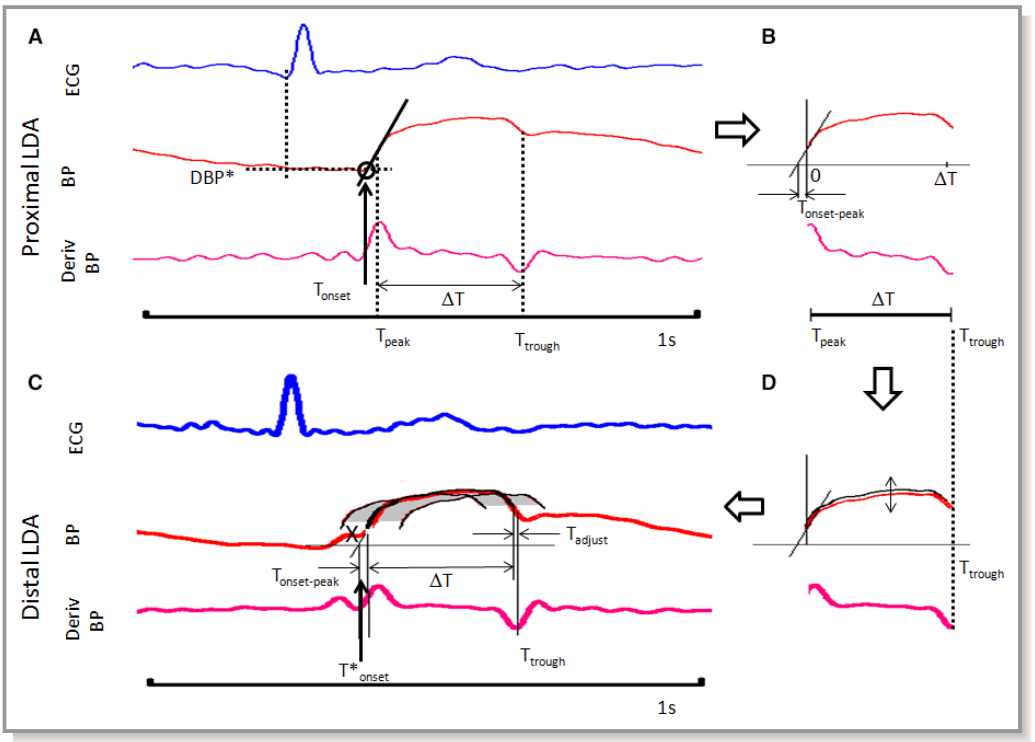

Figure 2. Detection of onset time of the blood pressure (BP) rise in the proximal and the distal positions of a coronary artery. A, For each cardiac cycle, the peak corresponding to the pressure rise and the trough corresponding to the dicrotic notch were detected in the first derivative of the BP at the times T_{peak} and T_{trough}, respectively. When the catheter was in the proximal position, the onset time (T_{onset}) of the BP rise was calculated for each cardiac cycle as the intersection of the tangent to the BP wave at T_{peak}, with the horizontal line passing through the preceding diastolic BP (DBP). To avoid the effect of microcirculation on the DBP, an extrapolated value (DBP*) was used, being equal to the value of the BP at the moment just before the onset of the R wave. B, A normalized BP wave was calculated for each cardiac cycle between T_{peak} and T_{trough} by subtracting from each BP sample the value of the preceding extrapolated DBP*. The average of all normalized BP waveforms in the proximal position resulted in an averaged normalized waveform of duration: $\Delta T = T_{trough} - T_{peak}$(time interval : $[0; \Delta T]$). The intersection of the tangent to the averaged normalized BP wave at time t=0 with the axis of abscissa was considered the averaged delay $T_{onset\text{-}peak}$ between T_{onset} of the BP and the peak of the pressure derivative. C, The averaged normalized waveform computed in the proximal position was superimposed on the normalized BP waveform of each cardiac cycle in the distal position by rescaling amplitude and synchronizing the last sample of the averaged waveform with the dicrotic notch time (T_{trough}) of the pressure waveform in the distal position. D, The root mean square error (RMSE) was calculated between the 2 superimposed waveforms. The averaged normalized waveform was shifted sample by sample with an interval of (−10;+10) ms to obtain a minimum value of the RMSE (time shift corresponding to the minimum of the RMSE [T_{adjust}]). Thus, the estimated onset time of the pressure rise for each cardiac cycle in the distal position is as follows: $T^*_{onset} = T_{trough} - \Delta T + T_{adjust} + T_{onset-peak}$. At 5 ms before T^*_{onset}, if the value of the BP ("X" on the BP trace) was lower than the extrapolated DBP*, T_{onset} of the pressure rise was obtained using the intersection of the tangent to the BP at T^*_{onset} with the horizontal line passing through the estimated DBP*. At 5 ms before T^*_{onset}, if the value of the BP was higher than the extrapolated DBP*, we considered that an artifactual premature pressure increase occurred before the pressure rise, and the tangent intersection method was not applicable, as it gave unreliable results: In this case, T_{onset} of the pressure rise was the estimated as T^*_{onset}. LDA indicates left descending artery.

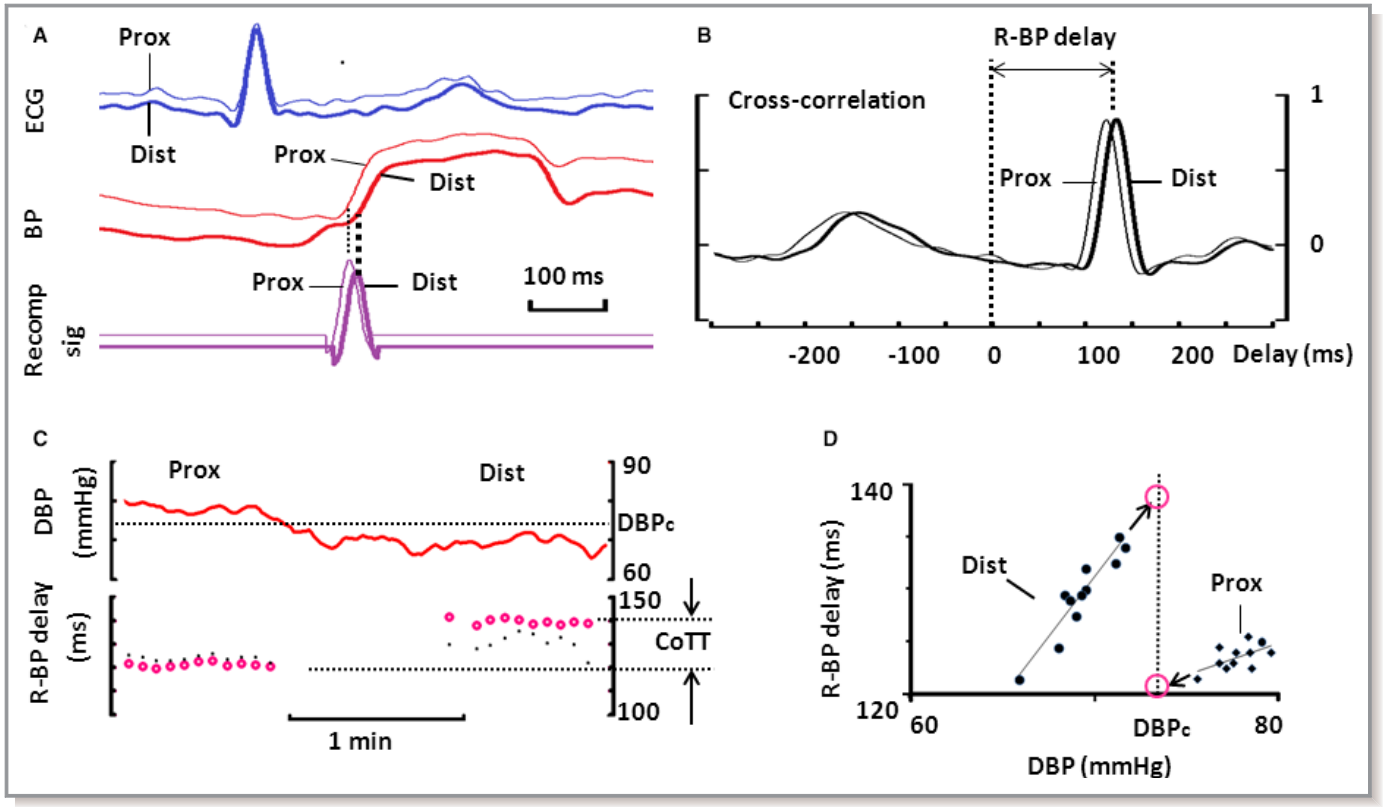

Figure 3. Delay between proximal and distal blood pressure (BP) wave fronts. A, Superimposed ECG, BP, and recomposed ECG signal for proximal and distal left descending artery (LDA), triggered by the R wave. The recomposed ECG signal was equal to the averaged R wave shape at the onset of the BP rise and zero elsewhere. B, Normalized cross-correlation between ECG and recomposed ECG signal in (A) for a ±300 ms shift range. The peak of the cross-correlation function corresponds to the delay between the R wave and the onset of the BP wave (R-BP delay). C, Time series of diastolic BP (DBP) and R-BP delays for adjacent periods containing 5 consecutive cardiac cycles in proximal and distal LDA. Both raw (dots) and extrapolated (open circles) R-BP delay time series are shown. The delay that the pressure wave needs to propagate from the proximal to the distal location (CoTT) is the difference of averaged extrapolated R-BP delays (arrows). D, Extrapolation of R-BP delay time series for a common DBP (DBP_c; mean of proximal and distal DBP), using linear regressions curves between R-BP delay and DBP. CoTT indicates coronary travel time; Dist, distal; Prox, proximal; Recomp, recomposed ECG signal.

wave and the onset of BP rise (R-BP delay). The cross-correlation function was applied for adjacent periods containing 5 consecutive R waves to smooth the influence of respiratory hemodynamic fluctuations. The maximum of this cross-correlation function corresponded to an averaged R-BP delay for the 5 consecutive R waves (Figure 3B). Computing of the cross-correlation function on adjacent groups of 5 consecutive R waves resulted in time series of R-BP delays $\Delta T_{R\text{-}BP}$ (Figure 3C). DBP was also averaged on 5 consecutive cardiac cycles, resulting in averaged DBP time series. A linear relationship was apparent in most patients between $\Delta T_{R\text{-}BP}$ and associated DBP time series for both proximal and distal positions (Figure 3D). Given this linear relationship, the time $\Delta T_{R\text{-}BP}$ series was extrapolated for a common DBP that was the mean of the proximal and distal DBPs (Figure 2). The extrapolated time series (ΔT^*_{R-BP}) was averaged for all 1-minute measurement periods in the proximal position ($Avg\Delta T^*_{R-BP\ prox}$) and in the distal position ($Avg\Delta T^*_{R-BP\ dist}$). The pulse wave front propagated from proximal to distal positions during the coronary travel time (CoTT) calculated as follows:

$$CoTT = Avg\Delta T^*_{R-BP\ dist} - Avg\Delta T^*_{R-BP\ prox}$$

CoPWV was calculated as coronary travel distance/CoTT and was expressed in m/s. For AoPWV measurement, the ECG-pressure delays were measured while the wire was at the level of the valsalva sinus and at the inlet of the brachiocephalic artery. As for CoPWV, the length of the wire externalized from the catheter when withdrawn from the distal to proximal positions represents the travel distance.

Statistical Analysis

Quantitative variables are summarized as mean±SD or numbers and percentages, as appropriate. Owing to a skewed distribution of CoPWV and AoPWV, a logarithmic transformation was performed before the statistical analysis. The

reproducibility of CoPWV was assessed using an intraclass correlation coefficient. Determinants of CoPWV and AoPWV were assessed by multivariable linear regression including univariate determinants in the model with $P<0.05$. Of note, conventional BP measurement was used for all statistical analyses. A paired Student *t* test was used to assess the effect of stenting within the same patients. Patients with an ACS or stable CAD were compared using the chi-square test, Fisher exact test, or the unpaired *t* test, as appropriate. Pearson correlation was used for comparing CoPWV and Aortic PWV. For CoPWV comparison, available measurements (1–3 measurements per patient, depending on the number of

Table 1. Patient Characteristics

Variable	All Patients (n=49)	Patients With Stable CAD (n=33)	Patients With ACS (n=16)	*P* Value*
Demographic characteristics				
Age, y	63.6±10.5	66.3±9.2	57.9±11.5	0.008
Men	39 (79.6)	24 (72.7)	15 (93.8)	0.14
Smoker	32 (65.3)	21 (63.6)	11 (68.8)	0.72
BMI, kg/m^2	27.3±5.4	28.3±6.0	25.2±3.3	0.06
Cardiac variables				
Heart rate, bpm	65.6±9.6	65.9±8.8	65±11.3	0.75
SBP, mm Hg	125.3±17.5	128.7±18.4	118.1±13.1	0.045
DBP, mm Hg	72.6±11.2	73.8±11.1	70.2±11.6	0.31
Medical history				
Diabetes mellitus	19 (38.8)	15 (45.5)	4 (25.0)	0.17
Hypertension	34 (69.4)	24 (72.7)	10 (62.5)	0.52
Dyslipidemia	33 (67.3)	25 (75.8)	8 (50.0)	0.07
CAD	27 (55.1)	21 (63.6)	6 (37.5)	0.09
Peripheral artery disease	7 (14.3)	5 (15.2)	2 (13.3)	0.62
Baseline treatment				
Angiotensin-converting enzyme inhibitor	29 (59.2)	18 (54.5)	11 (68.8)	0.34
Angiotensin II receptor blocker	5 (10.2)	4 (12.1)	1 (6.3)	0.52
Beta blocker	36 (73.5)	24 (72.7)	12 (75.0)	0.58
Calcium channel blocker	10 (20.4)	6 (18.2)	4 (25.0)	0.71
Statin	33 (67.3)	26 (78.8)	7 (43.8)	0.014
Oral antidiabetic drug	15 (30.6)	11 (33.3)	4 (25.0)	0.74
Insulin	9 (18.4)	6 (18.4)	3 (18.8)	0.96
Coronary angiography				
Radial approach	48 (98.0)	32 (97.0)	16 (100.0)	0.46
Number of diseased vessels				0.51
1	20 (40.8)	15 (45.5)	5 (31.3)	
2	18 (36.7)	12 (36.4)	6 (37.5)	
3	11 (22.4)	6 (18.2)	5 (31.3)	
Other variables				
eGFR, mL/min/1.73 m^2	79.4±22.4	78.0±19.8	82.3±27.5	0.54
LVEF, %	55.2±8.1	55.8±8.8	54.0±6.3	0.48

Values are mean±SD or n (%). ACS indicates acute coronary syndrome; BMI, body mass index; bpm, beats per minute; CAD, coronary artery disease; DBP, diastolic blood pressure; eGFR, estimated glomerular filtration rate; LVEF, left ventricular ejection fraction; SBP, systolic blood pressure.
*Difference across patients with stable CAD or an ACS using the chi-square test, Fisher exact test, or the unpaired *t* test.

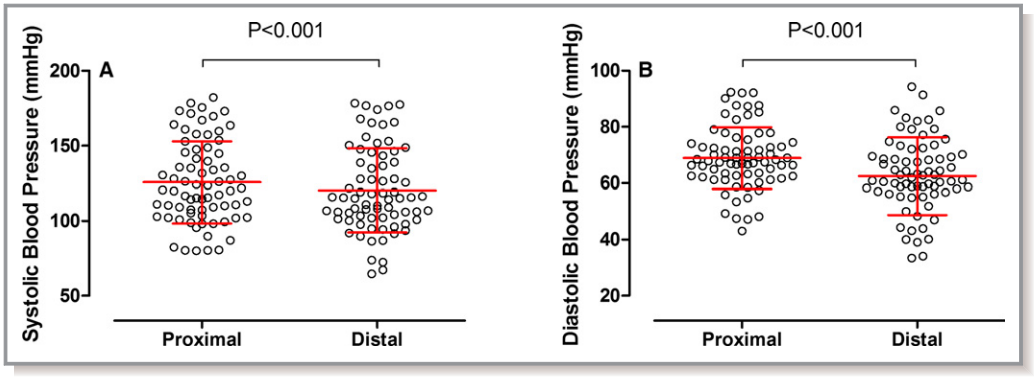

Figure 4. Systolic (A) and diastolic (B) coronary perfusion pressure at the proximal and distal sites.

vessels assessed) were averaged and used as the representative CoPWV for each patient. A sensitivity analysis was performed by comparing the CoPWV of the culprit vessel (ie, 1 vessel per patient) with the representative averaged CoPWV of the stable CAD subgroup. Analysis of covariance was used to provide adjusted means for PWV between patients with ACS and stable CAD. The analyses were performed using SPSS software 20.0.0 (IBM Corp). A value of $P<0.05$ was considered statistically significant.

Results

Patient Characteristics

Of the 53 patients considered, 4 were excluded (3 because of a poor ECG signal and 1 because of pressure artifacts). The population comprised 49 patients, 33 with stable CAD and 16 with an ACS.

The patient baseline characteristics are summarized in Table 1. As expected, a vast majority of patients were hypertensive with no difference in ongoing treatments except in the use of statins. Overall, 71 coronary arteries were analyzed in the 49 patients: 39 left descending artery, 23 right coronary artery, and 9 circumflex artery. Moreover, 24 of the 71 arteries were in patients with an ACS, with 15 of those arteries being culprit vessels (1 ACS patient had a recording only from a nonculprit artery), and 47 were in patients with stable CAD. Invasive coronary pressures are presented in Figure 4; they were significantly lower at the distal than at the proximal recording site ($P<0.001$ for all). No periprocedural complications occurred during CoPWV measurements. AoPWV was measured in 44 patients.

CoPWV and AoPWV Values

On average, CoPWV was 10.3±6.1 m/s, with no significant difference according to territory (10.0±6.6 m/s for left descending artery, 10.1±4.9 m/s for right coronary artery, and 12.4±7.1 m/s for circumflex artery; $P=0.55$). The reproducibility of CoPWV was fair, as assessed by the intraclass correlation coefficient (0.869, 95% CI 0.705–0.945; $P<0.001$). To allow for estimation of measurement precision, coronary travel distance and CoTT were presented separately (Figure 5). Given that the average travel distance was 11.6±2.46 cm, the absolute relative error was <2%. The time resolution for $\Delta T_{R\text{-}BP}$ due to sampling of ECG and BP was

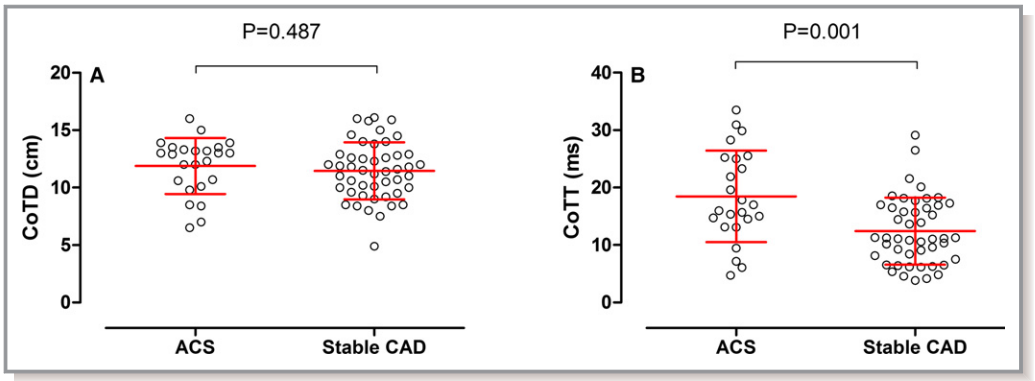

Figure 5. Difference in coronary travel distance (CoTD) (A) and coronary travel time (CoTT) (B) in patients with stable coronary artery disease (CAD) and an acute coronary syndrome (ACS).

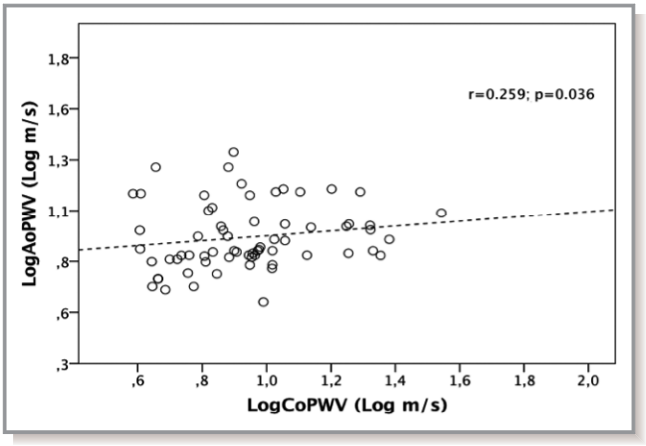

Figure 6. Correlation between coronary and aortic pulse wave velocities. AoPWV indicates aortic pulse wave velocity; CoPWV, coronary pulse wave velocity.

equal to the sampling period (Δt=1/2000 Hz=0.5 ms). Because CoTT is the difference between R-BP delays, its resolution was double the sampling period (ie, 1 ms). This led to an induced relative error for CoPWV <10% for t≥9 ms, which represents the majority of the recordings (average CoTT of 14.45±7.17 ms). The relative error increased to 17% in the few cases of short CoTT at 5 ms. In comparison, mean AoPWV was 8.73±3.74 m/s. A slight correlation was observed between CoPWV and AoPWV (r=0.259, P=0.036) (Figure 6). Carotid–femoral PWV was 9.6±2.8 m/s.

CoPWV and AoPWV Determinants

Table 2 shows the univariate and multivariable determinants of CoPWV and AoPWV. FFR, DBP, and a previous stent in the assessed artery were significant determinants of increased CoPWV. Adding renal function to the same set of variables did not substantially change the results (data not shown). As shown in Figure 7A, a marked increase in CoPWV was observed after stent implantation (during the same procedure) in 33 patients, from 9.7±5 to 17.1±9.01 m/s (P<0.001). For AoPWV, the only significant determinant in univariate and multivariable analysis was age, whereas a trend for a positive association was found with systolic BP in univariate analysis only (Table 2).

ACS Versus Stable CAD

Mean CoPWV was lower in patients with an ACS patients than stable CAD (7.6±3 versus 11.8±6.6 m/s; P=0.012) (Figure 7B). This difference remained after removal of an outlier in the stable CAD group (P=0.016). The difference in CoPWV was mostly due to a difference in CoTT, whereas coronary travel distance was similar between the 2 groups (Figure 5). Considering only the right coronary artery, CoPWV remained lower in ACS than CAD vessels (6.9±2.5 versus 12±5 m/s, respectively; P=0.004). The same trend was observed for the left descending artery (7.5±4.8 versus 10.9±7 m/s for ACS and stable CAD, respectively; P=0.08). The circumflex arteries were not included in this analysis because of their small sample size. When considering only ACS culprit vessels versus stable CAD, the difference was even more marked (6.5±2.2 versus 11.5±6.4 m/s; P=0.001). These differences also remained (P=0.037) after adjustment for the characteristics that differed between patients with stable CAD and ACS (ie, age, systolic BP, statin use) (Table 1). When further adjusting for all cardiovascular risk factors, CoPWV remained different between the 2 groups (P=0.046).

In comparison, a trend of difference was observed between ACS and stable CAD patients concerning AoPWV (7.3±3.2 versus 9.5±3.8 m/s, respectively; P=0.065). After adjustment for differences between ACS and stable CAD patients, the difference was even less marked (P=0.2). This was also true for carotid–femoral PWV (9.8±3.3 versus 9.5±2.5 m/s; P=0.8).

The average severity of coronary stenosis did not differ between patients with ACS and stable CAD (hyperemia FFR values: 0.77±0.08 versus 0.78±0.09, respectively; P=0.842), and a similar proportion of patients had FFR values <0.8 (66.7% versus 68.1%, respectively; P=0.554).

Discussion

We described a method for measuring CoPWV that involves a regular pressure wire and dedicated software. With this approach, we demonstrated—for the first time—a noticeable difference in CoPWV between stable and unstable coronary vessel diseases. No such difference was apparent for AoPWV. CoPWV may prove to be a relevant assessment of instability in coronary vessels.

Determination of CoPWV was based on asynchronous pressure recordings gated on an ECG because synchronous recordings would have required placing 2 pressure wires in the coronary arteries, which is both unethical and not applicable in routine clinical practice. Accurate determination of the wave front was mandatory, requiring rigorous analysis of the signal. The characteristic points are usually chosen near the foot (ie, the nadir) of the pressure waveform,[14] which is believed to be relatively free of arterial wave reflections, so the interference with the calculation of forward wave velocity is minimized. In our study, we used the tangent intersection method, currently regarded as the best technique for proximal wave detection.[14] In the distal part of the artery, this technique was often compromised by a premature pressure rise, probably due to myocardial contraction. In this context, our approach was based on detection of the dicrotic notch

Table 2. Determinants of Increased Coronary and Aortic Pulse Wave Velocity in Univariate and Multivariate Analysis

	CoPWV (m/s), n=49				AoPWV (m/s), n=44			
	Univariate		Multivariable*		Univariate		Multivariable*	
Determinant	β	*P* Value	β	*P* Value	β	*P* Value	β	*P* Value
Age	0.009	0.94	—	—	0.429	0.004	0.344	0.020
Sex (F=0; M=1)	0.051	0.67	—	—	−0.212	0.17	—	—
Hypertension (N=0; Y=1)	0.047	0.70	—	—	0.297	0.05	0.139	0.34
Diabetes mellitus (N=0; Y=1)	−0.010	0.94	—	—	0.230	0.13	—	—
Smoking (N=0; Y=1)	0.243	0.041	0.196	0.064	−0.223	0.15	—	—
Dyslipidemia (N=0; Y=1)	0.090	0.46	—	—	0.247	0.11	—	—
BMI (+1 kg/m²)	0.260	0.028	0.164	0.142	−0.002	0.99	—	—
History of CAD (N=0; Y=1)	0.145	0.23	—	—	0.183	0.24	—	—
PAD (N=0; Y=1)	−0.031	0.80	—	—	0.169	0.27	—	—
Previous stent (N=0; Y=1)	0.373	0.001	0.247	0.036	—	—	—	—
Number of diseased vessels (+1)	−0.115	0.34	—	—	−0.068	0.66	—	—
Renal function (+1 mL/min)	0.231	0.05	—	—	−0.275	0.07	—	—
ACEI (N=0; Y=1)	0.089	0.46	—	—	−0.056	0.72	—	—
ARB (N=0; Y=1)	−0.047	0.70	—	—	0.238	0.12	—	—
Beta blocker (N=0; Y=1)	0.177	0.14	—	—	0.142	0.36	—	—
CCB (N=0; Y=1)	−0.075	0.54	—	—	0.077	0.62	—	—
Statin (N=0; Y=1)	0.278	0.019	0.026	0.836	0.186	0.23	—	—
Oral antidiabetic drug (N=0; Y=1)	0.126	0.29	—	—	0.345	0.022	0.234	0.11
Insulin (N=0; Y=1)	−0.155	0.20	—	—	−0.018	0.91	—	—
SBP (+1 mm Hg)	0.178	0.14	—	—	0.280	0.07	—	—
DBP (+1 mm Hg)	0.334	0.004	0.280	0.01	−0.009	0.96	—	—
Heart rate (+1 bpm)	−0.067	0.58	—	—	0.087	0.57	—	—
FFR (0=FFR >0.8; 1=FFR ≤0.8)	−0.355	0.002	−0.265	0.012	—	—	—	—
LVEF (+1%)	−0.200	0.10	—	—	−0.151	0.34	—	—

ACEI indicates angiotensin-converting enzyme inhibitor; AoPWV, aortic pulse wave velocity; ARB, angiotensin II receptor blocker; BMI, body mass index; bpm, beats per minute; CAD, coronary artery disease; CCB, calcium channel blocker; CoPWV, coronary pulse wave velocity; DBP, diastolic blood pressure; F, female; FFR, fractional flow reserve; LVEF, left ventricular ejection fraction; M, male; N, no; PAD, peripheral artery disease; SBP, systolic blood pressure; Y, yes.
*Adjusted for all variables with $P<0.05$ in univariate analysis.

(trough in the BP-derivative signal). The dicrotic notch is a suitable time reference point for PWV determination, as an alternative to the systolic foot in the carotid artery,[15] but it was not sufficiently precise per se in the context of coronary arteries. Consequently, we used it to trigger a memorized BP waveform in the proximal position; a curve fitting between the proximal and distal BP waveform shapes was applied to improve the detection of the distal waveform. To take into account pressure variation that may occur between the proximal and distal parts of the artery, an adjustment on DBP was made within each coronary artery. Finally, we used high-frequency sampling to increase the precision of the measurement. A few attempts have been made to measure CoPWV, but the methods used (eg, the single-point method) are questionable for the coronary circulation, characterized by short vessels, multiple sources of waves, and changing peripheral resistance during each cardiac cycle.[12,16] Moreover, reproducibility was not assessed in previous CoPWV assessments, and BP variations along the coronary vessel were not taken into account. Conversely, several aspects validate our method in the absence of a gold standard. First, it provides CoPWV values similar to those obtained in dogs[9] and humans.[12] Second, when applied to the aorta, it provides values within the expected range.[17] Third, it can detect the stiffening effect of stenting, demonstrated in other arteries.[18] Fourth, it has good reproducibility. This method has the advantage of evaluating the global mechanical property of an artery, which may be better than previous methods using

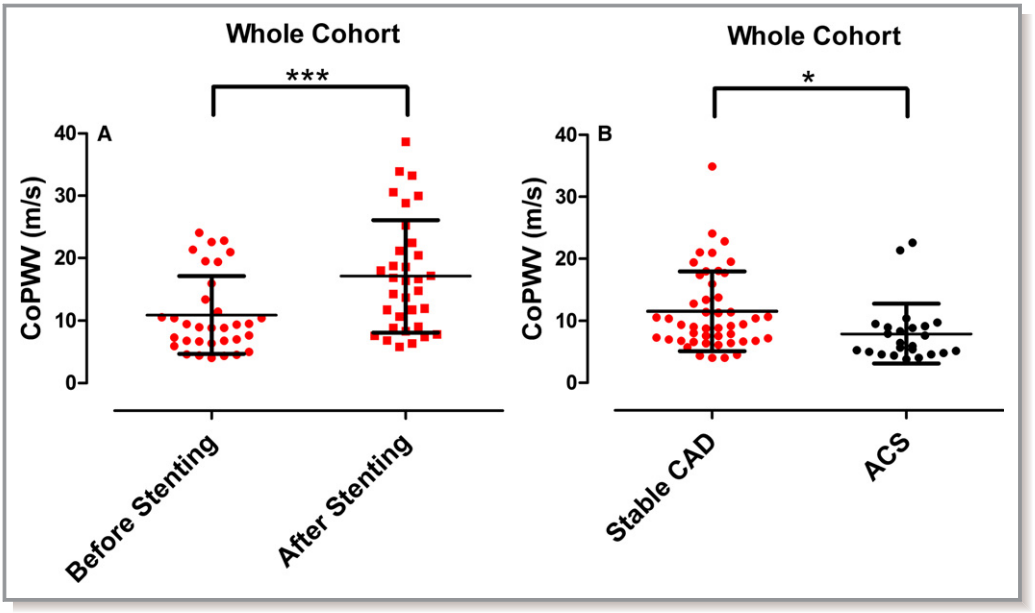

Figure 7. Coronary pulse wave velocity (CoPWV) (A) before and after stenting and (B) in patients with stable coronary artery (CAD) disease or an acute coronary syndrome (ACS). Dots indicate individual recordings, and whiskers represent means and standard deviations. *P=0.012; ***P<0.001.

intravascular ultrasound.[7] Indeed, it seems challenging, given methodological constraints, to precisely determine the variation in diameter between systole and diastole in a coronary artery because of the swing of the heart.

Clinical Relevance of CoPWV

Coronary compliance likely influences several features of myocardial perfusion and plaque complications. It may also represent a potential early marker of endothelial dysfunction and future atherosclerosis.[19] More importantly, it has been suggested as a reliable marker of high-risk plaques.[6] Our results are perfectly in line with this hypothesis, as CoPWV was a marker of vessel vulnerability. To our knowledge, this is the first time that such a difference has been reported; previous attempts to measure CoPWV were performed only in angiographically normal vessels.[12] This difference of CoPWV between ACS and stable CAD vessels was explained mostly by a difference in CoTT. The 6-ms average CoTT difference exceeded the precision of the measurement, which makes the difference of CoPWV between ACS and stable CAD compelling. This finding was also strengthened by the fact that it was verified for the right coronary and left descending arteries considered separately and by the fact that it remained after several adjustments for potential confounders. The degree of stenosis was not different between ACS and stable CAD and did not account for the difference in CoPWV. A major additional finding and strength of our study is that this difference cannot be accounted for by a "vascular aging effect." Indeed, AoPWV and carotid–femoral PWV were not significantly different for patients with unstable and stable disease. In addition, the determinants of AoPWV and CoWPV were not the same, and both were only slightly correlated, in keeping with what has been reported previously for elastic and muscular arteries.[20] Matrix degradation intervenes at the level of a vulnerable plaque, with a shift in the ratio of collagen[21,22] affecting the local elastic properties of coronary arteries, as described by intravascular ultrasound.[7] It is possible that these structural differences between unstable and stable plaques led to detectable differences in global vessel compliance and thus in CoPWV. However, high coronary compliance may also be a determinant of plaque rupture by increasing cyclic stretch. In this respect, an important point to consider is the relation between the aorta and the coronary arteries in terms of compliance because they are in close proximity. It is well established that there is a physiological stiffness gradient between the aorta and peripheral muscular arteries. This impedance mismatch is protective of the microcirculation because it prevents the transmission of forward-traveling pressure (by generating a reflected wave).[5] It fits with what was observed in stable CAD patients because CoPWV was markedly higher than AoPWV. Rolandi et al also reported CoPWV values that were ≈32% higher than those for AoPWV,[12] fueling the hypothesis of a protective mismatch. Conversely, the similar PWV values between the aorta and the coronary artery found in ACS may shift the compliance mismatch more distally in the coronary tree and provoke plaque rupture and ACS in the presence of a

vulnerable plaque.[6] This hypothesis is consistent with the fact that the majority of ACS events concerned the proximal third of the artery,[23] a segment that is probably exposed to high cyclic stretch. Fortier et al recently found that aortic–brachial stiffness mismatch was predictive of mortality in a dialysis population.[24] Our data roughly suggest a similar conclusion, namely, that the aortic–coronary stiffness mismatch may play a role in the occurrence of acute coronary events. Prospective studies, however, are needed to evaluate the prognostic impact of coronary compliance.

Another major effect detected by CoPWV, albeit expected, is that of stenting. This is in line with the increased AoPWV occurring after abdominal aorta stenting reported by our group.[18] Although a metal stent is expected to impair the compliance of an elastic artery, this has never been described in coronary arteries.

Limitations

The patient groups are of moderate size; however, the results were highly statistically significant. Assessments of CoPWV were not available in 4 patients because of artifacts, but improvements in the technique should resolve this point. Hemodynamics and transmural pressure may change between measurements in the catheterization laboratory and between patients; however, patients with heart failure were excluded, and an adjustment for DBP was made to avoid this bias. Measurement of coronary artery length is challenging. It was carefully determined when the wire was pulled outside the guiding catheter, but some errors are still possible. CoPWV values in nondiseased vessels are unknown because it does not seem ethical to perform such measurement in patients. Nevertheless, the fact that both groups (ie, stable and unstable disease) had established cardiovascular disease prevents an important bias in testing the association of CoPWV with vessel vulnerability. With respect to clinical utility, this technique is not appropriate for general population screening because of its invasive nature; however, it could be supplemental to a coronary angiogram to risk-stratify a plaque.

Perspectives

Vascular stiffness has an important prognostic impact. Although aortic stiffness is the parameter generally assessed, local stiffness may be more specific. At the coronary level, we described a safe method to measure CoPWV that can be used in routine practice during a coronary angiography. CoPWV seems to be lower in patients with ACS, but its prognostic consequences must be determined in dedicated prospective trials. This technique paves the way for a new field of research to better understand the pathophysiology of plaque complications and to better risk-stratify patients.

Acknowledgments

We would like to remember Professor Giampiero Bricca for his contribution to the design of this study.

Disclosures

None.

References

1. Harbaoui B, Courand PY, Milon H, Fauvel JP, Khettab F, Mechtouff L, Cassar E, Girerd N, Lantelme P. Association of various blood pressure variables and vascular phenotypes with coronary, stroke and renal deaths: potential implications for prevention. *Atherosclerosis*. 2015;243:161–168.
2. Laurent S, Boutouyrie P, Asmar R, Gautier I, Laloux B, Guize L, Ducimetiere P, Benetos A. Aortic stiffness is an independent predictor of all-cause and cardiovascular mortality in hypertensive patients. *Hypertension*. 2001;37:1236–1241.
3. Ben-Shlomo Y, Spears M, Boustred C, May M, Anderson SG, Benjamin EJ, Boutouyrie P, Cameron J, Chen CH, Cruickshank JK, Hwang SJ, Lakatta EG, Laurent S, Maldonado J, Mitchell GF, Najjar SS, Newman AB, Ohishi M, Pannier B, Pereira T, Vasan RS, Shokawa T, Sutton-Tyrell K, Verbeke F, Wang KL, Webb DJ, Willum Hansen T, Zoungas S, McEniery CM, Cockcroft JR, Wilkinson IB. Aortic pulse wave velocity improves cardiovascular event prediction: an individual participant meta-analysis of prospective observational data from 17,635 subjects. *J Am Coll Cardiol*. 2014;63:636–646.
4. Laurent S, Briet M, Boutouyrie P. Large and small artery cross-talk and recent morbidity-mortality trials in hypertension. *Hypertension*. 2009;54:388–392.
5. Safar ME, Blacher J, Jankowski P. Arterial stiffness, pulse pressure, and cardiovascular disease-is it possible to break the vicious circle? *Atherosclerosis*. 2011;218:263–271.
6. Chatzizisis YS, Giannoglou GD. Coronary hemodynamics and atherosclerotic wall stiffness: a vicious cycle. *Med Hypotheses*. 2007;69:349–355.
7. Jeremias A, Spies C, Herity NA, Pomerantsev E, Yock PG, Fitzgerald PJ, Yeung AC. Coronary artery compliance and adaptive vessel remodelling in patients with stable and unstable coronary artery disease. *Heart*. 2000;84:314–319.
8. Vlachopoulos C, Xaplanteris P, Aboyans V, Brodmann M, Cifkova R, Cosentino F, De Carlo M, Gallino A, Landmesser U, Laurent S, Lekakis J, Mikhailidis DP, Naka KK, Protogerou AD, Rizzoni D, Schmidt-Trucksass A, Van Bortel L, Weber T, Yamashina A, Zimlichman R, Boutouyrie P, Cockcroft J, O'Rourke M, Park JB, Schillaci G, Sillesen H, Townsend RR. The role of vascular biomarkers for primary and secondary prevention. A position paper from the European Society of Cardiology Working Group on peripheral circulation: endorsed by the Association for Research into Arterial Structure and Physiology (ARTERY) Society. *Atherosclerosis*. 2015;241:507–532.
9. Arts T, Kruger RT, van Gerven W, Lambregts JA, Reneman RS. Propagation velocity and reflection of pressure waves in the canine coronary artery. *Am J Physiol*. 1979;237:H469–H474.
10. Aguado-Sierra J, Parker KH, Davies JE, Francis D, Hughes AD, Mayet J. Arterial pulse wave velocity in coronary arteries. *Conf Proc IEEE Eng Med Biol Soc*. 2006;1:867–870.
11. Davies JE, Whinnett ZI, Francis DP, Willson K, Foale RA, Malik IS, Hughes AD, Parker KH, Mayet J. Use of simultaneous pressure and velocity measurements to estimate arterial wave speed at a single site in humans. *Am J Physiol Heart Circ Physiol*. 2006;290:H878–H885.
12. Rolandi MC, De Silva K, Lumley M, Lockie TP, Clapp B, Spaan JA, Perera D, Siebes M. Wave speed in human coronary arteries is not influenced by microvascular vasodilation: implications for wave intensity analysis. *Basic Res Cardiol*. 2014;109:405.
13. Girerd N, Legedz L, Paget V, Rabilloud M, Milon H, Bricca G, Lantelme P. Outcome associations of carotid-femoral pulse wave velocity vary with different measurement methods. *Am J Hypertens*. 2012;25:1264–1270.
14. Chiu YC, Arand PW, Shroff SG, Feldman T, Carroll JD. Determination of pulse wave velocities with computerized algorithms. *Am Heart J*. 1991;121:1460–1470.
15. Hermeling E, Reesink KD, Kornmann LM, Reneman RS, Hoeks AP. The dicrotic notch as alternative time-reference point to measure local pulse wave velocity in the carotid artery by means of ultrasonography. *J Hypertens*. 2009;27:2028–2035.

16. Kolyva C, Spaan JA, Piek JJ, Siebes M. Windkesselness of coronary arteries hampers assessment of human coronary wave speed by single-point technique. *Am J Physiol Heart Circ Physiol*. 2008;295:H482–H490.
17. Determinants of pulse wave velocity in healthy people and in the presence of cardiovascular risk factors: 'Establishing normal and reference values'. *Eur Heart J*. 2010;31:2338–2350.
18. Lantelme P, Dzudie A, Milon H, Bricca G, Legedz L, Chevalier JM, Feugier P. Effect of abdominal aortic grafts on aortic stiffness and central hemodynamics. *J Hypertens*. 2009;27:1268–1276.
19. Cohn JN, Duprez DA, Grandits GA. Arterial elasticity as part of a comprehensive assessment of cardiovascular risk and drug treatment. *Hypertension*. 2005;46:217–220.
20. Zhang Y, Agnoletti D, Protogerou AD, Topouchian J, Wang JG, Xu Y, Blacher J, Safar ME. Characteristics of pulse wave velocity in elastic and muscular arteries: a mismatch beyond age. *J Hypertens*. 2013;31:554–559; discussion 559
21. Moreno PR, Falk E, Palacios IF, Newell JB, Fuster V, Fallon JT. Macrophage infiltration in acute coronary syndromes. Implications for plaque rupture. *Circulation*. 1994;90:775–778.
22. Virmani R, Kolodgie FD, Burke AP, Farb A, Schwartz SM. Lessons from sudden coronary death: a comprehensive morphological classification scheme for atherosclerotic lesions. *Arterioscler Thromb Vasc Biol*. 2000;20:1262–1275.
23. Wang JC, Normand SL, Mauri L, Kuntz RE. Coronary artery spatial distribution of acute myocardial infarction occlusions. *Circulation*. 2004;110:278–284.
24. Fortier C, Mac-Way F, Desmeules S, Marquis K, De Serres SA, Lebel M, Boutouyrie P, Agharazii M. Aortic-brachial stiffness mismatch and mortality in dialysis population. *Hypertension*. 2015;65:378–384.